

Complete excitation spectrum for a charge-density-wave system

M. S. Sherwin and A. Zettl

Department of Physics, University of California, Berkeley, Berkeley, California 94720

P. L. Richards

Department of Physics, University of California, Berkeley, California 94720

and Materials and Chemical Sciences Division, Lawrence Berkeley Laboratory, Berkeley, California 94720

(Received 7 August 1987)

We report measurements of the far-infrared (FIR) reflectance of the charge-density-wave (CDW) conductor $(\text{TaSe}_4)_2\text{I}$. In the CDW state, and for incident electric field polarized parallel to the crystal chain direction, the associated FIR conductivity shows a giant resonance at 38 cm^{-1} . Our results, when combined with previous measurements at lower and higher frequencies, provide the first consistent and complete excitation spectrum of a CDW system. We propose that a giant FIR mode distinct from the pinned CDW mode is a generic feature of CDW systems.

Over the past 15 years, far-infrared (FIR) spectroscopy has been an invaluable tool for the study of quasi-one-dimensional materials that undergo a Peierls transition to the charge-density-wave (CDW) state.¹⁻³ Based on the theory of Lee, Rice, and Anderson (LRA),⁴ one expects a large ir-active response due to the pinned mode of the CDW at frequencies low compared to ordinary phonons and electronic excitations. Large oscillator strength has been found in both the FIR (Refs. 1-3) and microwave⁵⁻⁷ frequency ranges in several CDW systems. In both frequency ranges, part of this oscillator strength has been attributed to the pinned mode of the CDW. Unfortunately, FIR and microwave measurements reported to date have not provided a complete and consistent dielectric function in the millimeter and submillimeter wave region, and it is not yet clear whether the FIR and microwave modes are distinct. In this Rapid Communication, we present FIR data that unambiguously show that, in the CDW material $(\text{TaSe}_4)_2\text{I}$, the microwave and FIR modes are distinct. Therefore, the assignment of giant FIR modes observed in other CDW materials to the pinned mode must be reexamined.

We have measured the reflectance of $(\text{TaSe}_4)_2\text{I}$ for frequencies from 8 to 350 cm^{-1} and temperatures from 10 to 290 K. The sample used for these measurements was a mosaic of several single crystals carefully oriented along both principal axes. The crystals were grown in our laboratory and had faces that were typically $2 \times 5 \text{ mm}^2$. The sample was placed in a continuous transfer helium cryostat adapted in our laboratory for use with a Michelson Fourier spectrometer to measure polarized reflectance. Radiation was detected using a low-noise composite bolometer operated at 1.5 K. At each fixed sample temperature, the sample spectrum was normalized to that of a polished brass plug. After all data had been measured, gold was evaporated onto (only) the crystal faces of the mosaic and the reflectance of the sample was again normalized to that of the brass. The details of the experimental technique will be described elsewhere.⁸

Reflectance curves for $(\text{TaSe}_4)_2\text{I}$ at various temperatures, for radiation polarized parallel to the c axis, are

presented in Fig. 1. At room temperature the reflectance is high and fairly featureless except for a slow decrease with increasing frequency from 0.9 at 30 cm^{-1} to 0.7 at 300 cm^{-1} . As the sample is cooled through the Peierls transition temperature $T_p = 265 \text{ K}$, the reflectance between 30 and 90 cm^{-1} begins to increase, and the decrease in the reflectance near 100 cm^{-1} begins to sharpen. These changes signal the onset of an ir active mode associated with the CDW. As the sample is cooled further, the decrease in reflectance develops into an extremely sharp edge, with the reflectance at 110 K dropping from unity at 92 cm^{-1} to 0.2 at 96 cm^{-1} . The reflectance changes little between 110 K and 10 K. Figure 2 (solid line) shows the measured reflectance at 10 K. The reflectance rises from 0.9 at low frequencies to near unity at 40 cm^{-1} and remains near unity until 94 cm^{-1} , with the exception of a small dip at 79 cm^{-1} . At frequencies beyond the reflectance edge, two sharp features are evident, at 143 and 190 cm^{-1} . Between 200 and 350 cm^{-1} the reflectance slowly rises with no additional sharp features and then levels off at a value of 0.6, consistent with higher frequency measurements.⁹

Reflectance was also measured perpendicular to the c

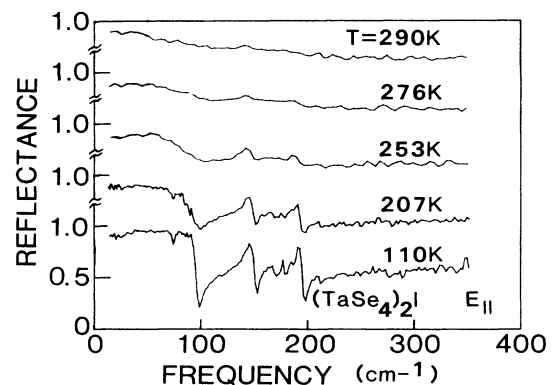


FIG. 1. FIR reflectance of $(\text{TaSe}_4)_2\text{I}$ at selected temperatures.

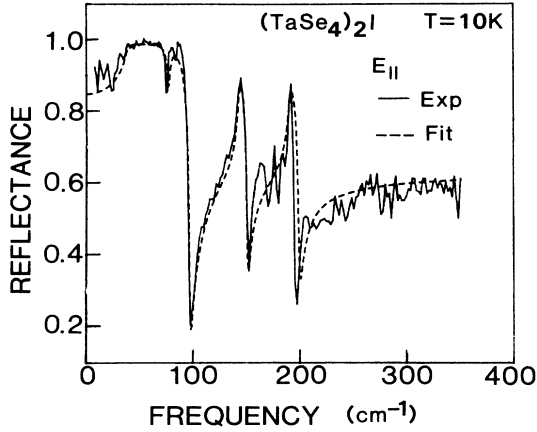


FIG. 2. FIR reflectance of $(\text{TaSe}_4)_2\text{I}$ at 10 K (solid line) and oscillator fit (dashed line) to that reflectance calculated from the parameters of Table I.

axis in $(\text{TaSe}_4)_2\text{I}$ at various temperatures above and below T_p . As expected for this quasi-one-dimensional material, the perpendicular spectrum shares no common features with the parallel spectrum described above.⁸

The pattern of a rise in the reflectance from 0.9 to 20 cm^{-1} to near unity above 40 cm^{-1} followed by a reflectance edge suggests the presence of a mode with a giant oscillator strength in the region between 25 and 50 cm^{-1} . Transmittance measurements⁸ on a sample of order 100 μm thick show a transmittance that decreases from 5% at 10 cm^{-1} to $<0.5\%$ above 40 cm^{-1} , also suggesting the presence of such a mode. The other peaks in the spectrum (for example, at 143 and 190 cm^{-1}) indicate modes with much smaller oscillator strength. In order to extract the complex dielectric function $\epsilon = \epsilon_1 + i\epsilon_2$ from the reflectance data, we have fitted the reflectance to a model with four Lorentz oscillators and a background dielectric constant $\epsilon_\infty = 75$:

$$\epsilon_1(f) = \epsilon_\infty + \sum_n \frac{S_n [1 - (f/f_{0n})^2]}{[1 - (f/f_{0n})^2]^2 + f^2/f_{0n}^4 \tau_n^2}, \quad (1)$$

$$\epsilon_2(f) = \sum_n \frac{(S_n/f_{0n} \tau_n) f/f_{0n}}{[1 - (f/f_{0n})^2]^2 + f^2/f_{0n}^4 \tau_n^2}, \quad (2)$$

where the resonant frequency, oscillator strength, and damping time of the n th mode are respectively f_{0n} , $S_n(2\pi f_{0n})^2$, and τ_n .

The dashed line in Fig. 2 shows the fit to the reflectance computed from the model dielectric function. This dielectric function is dominated by a mode with $f_0 = 38 \text{ cm}^{-1}$, $S_0 \tau_0 = 13$, and $S = 500$. Changes in the parameters of the 38 cm^{-1} mode of only 5% visibly degrade the quality of the fit. The three other modes used have had respectively $f_0 = 79, 149, \text{ and } 194 \text{ cm}^{-1}$; $f_0 \tau = 25, 50, \text{ and } 50$; and $S = 1.5, 2.5, \text{ and } 4$. Our fit is not at all sensitive to the existence of a mode with $S = 10^4$ at 35 GHz, as observed using microwave techniques.⁶ This proves that our data are consistent with lower-frequency measurements.

Figure 3 shows ϵ_1 and ϵ_2 calculated from Eqs. (1) and (2) using the fitted parameters. Peaks in ϵ_2 (and hence the conductivity) occur at each of the mode frequencies,

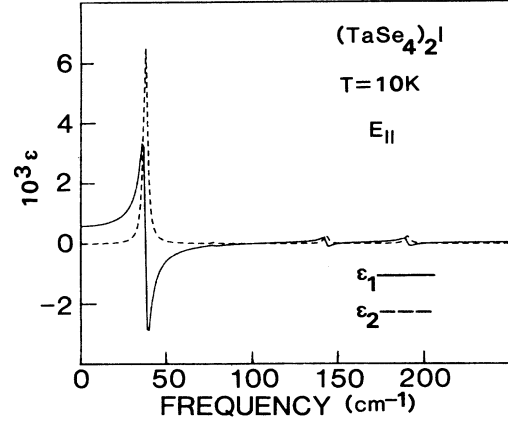


FIG. 3. Complex dielectric function $\epsilon = \epsilon_1 + i\epsilon_2$ for $(\text{TaSe}_4)_2\text{I}$ at 10 K, as determined by the oscillator fit to the reflectivity. Both ϵ_1 and ϵ_2 are flat and featureless between 250 and 400 cm^{-1} .

the largest being at 38 cm^{-1} . At frequencies much less than the 38 cm^{-1} resonance peak, ϵ_1 of Fig. 3 is approximately equal to 600, which is consistent with the high reflectance at low FIR frequencies. Between 38 and 100 cm^{-1} , the dielectric function is negative, giving rise to the near unit, reflectance over this frequency range. The small dip at 79 cm^{-1} results from a weak mode at that frequency. At 100 cm^{-1} , the dielectric function crosses the real axis, leading to the sharp reflectance edge observed in Fig. 2.

Our measurement of the FIR spectrum of $(\text{TaSe}_4)_2\text{I}$ completes the excitation spectrum for this material, and for the first time we have a complete and consistent dielectric response function from dc to the Peierls gap of a sliding CDW compound. The contributions to the dielectric function in the CDW state are as follows. A broad peak with a temperature-dependent frequency¹⁰ appears below 1 MHz and has been associated with dielectric relaxation of the CDW. A large, underdamped resonance⁶ at 35 GHz = 1.2 cm^{-1} has been convincingly attributed to the pinned mode of the CDW. At 38 cm^{-1} we have observed the giant FIR resonance described above. From 78 to 194 cm^{-1} we observe a number of weak, sharp resonances which we associate with ordinary phonons. Finally, the Peierls gap has been observed⁹ near 2000 cm^{-1} . Table I is a summary of the principal features of the dielectric functions of $(\text{TaSe}_4)_2\text{I}$, $\text{K}_{0.3}\text{MoO}_3$, and NbSe_3 .

A giant FIR resonance^{1,3} at 15 cm^{-1} , similar to that in $(\text{TaSe}_4)_2\text{I}$, has been reported in $\text{K}_{0.3}\text{MoO}_3$. The FIR resonance was originally assigned to the pinned mode.¹ However, the presence of a distinct mode near 3 cm^{-1} was later deduced³ by combining 40-K microwave⁷ and 2-K FIR data.³ The assignment of the 3 cm^{-1} mode to the pinned mode³ is consistent with assignments for the microwave modes in other CDW materials.^{5,6}

In NbSe_3 , the pinned mode appears at microwave frequencies⁵ as an extremely overdamped mode with width 60 GHz. A large temperature-dependent reflectance edge² similar to that in Fig. 1 has also been observed at 140 cm^{-1} and has been interpreted as arising from a combination of free carriers and the pinned mode. However,

TABLE I. Dielectric response of CDW's for frequencies up to the Peierls gap.

	Radio frequency: Dielectric relaxation ^a (MHz)	Microwave: Pinned phason ^b (GHz)	Far infrared: Optical phason? ^c (cm ⁻¹)	Near infrared: Peierls gap ^d (cm ⁻¹)
(TaSe ₄) ₂ I	0.2	35	38	2000
K _{0.3} MoO ₃	0.7	84	15	1200
NbSe ₃	19	4.3	< 140?	560

^aReference 10.

^b(TaSe₄)₂I: Ref. 6; NbSe₃: Ref. 5; K_{0.3}MoO₃: Ref. 3.

^cK_{0.3}MoO₃: Refs. 1 and 3; NbSe₃: Ref. 2.

^d(TaSe₄)₂I: Ref. 9; K_{0.3}MoO₃: Ref. 1; NbSe₃: Tunneling measurement of A. Fournel, J. P. Sorbier, M. Konczykowski, and P. Monceau, Phys. Rev. Lett. **57**, 2199 (1986). Reference 2 reports a value of 190 cm⁻¹.

the parameters for the pinned mode extracted under this interpretation are inconsistent with the microwave data. A possibility that should be investigated is that the 140 cm⁻¹ edge arises from a combination of free carriers and a giant FIR mode.

In the seminal work on the excitation spectrum of CDW's, Lee, Rice, and Anderson⁴ predicted two branches of excitations for a CDW: an acoustic or phason branch consisting of excitations of the phase of the CDW, and an optical or amplitudon branch consisting of excitations of the CDW amplitude. In the theory of LRA, the zero wave vector phason is totally antisymmetric and hence is only active, while the zero wave vector amplitudon is totally symmetric and hence only Raman active. The presence of *two* ir active modes of the CDW with large oscillator strength in (TaSe₄)₂I requires a modification of this classic picture.

A second ir active mode that is generic to CDW systems is the optical phason, also called by Walker¹¹ the first-harmonic phason. The optical phason may be simply understood if one draws a parallel between the modulated electronic density in a CDW and the more familiar case of alternating positive and negative ions in an ionic crystal such as NaCl. In this analogy, the $q=0$ acoustic phason corresponds to translations of the earlier NaCl crystal, the amplitudon would correspond to a mode in which charge is transferred between Na and Cl ions, and the optical phason would correspond to the familiar ir active optic mode of NaCl. In the same way one would calculate the frequency of the zone center optic phonon mode in a 1D diatomic crystal with nearest-neighbor interactions, one can estimate the frequency of the optical phason from the slope of the dispersion relation and the CDW wave vector $2k_F$. The slope of the acoustic phason branch is given by LRA as $v_{ph} = \sqrt{(m/m^*)}v_F$, where m is the band mass, m^* the Frohlich mass, and v_F the Fermi velocity. We assume m =free electron mass, $m^*/m=10^4$ from microwave measurements,⁶ $v_F = \hbar k_F/m$, and $2k_F = 2\pi/14 \text{ \AA}$ from x-ray measurements.¹² The calculated frequency of

the optical phason is then $(2/\pi)(2k_F v_{ph}/2\pi) = 39 \text{ cm}^{-1}$, remarkably close to the 38 cm⁻¹ resonant frequency derived from our measurements.

We cannot exclude the possibility that other modes folded to the zone center by the CDW distortion could give rise to the 38 cm⁻¹ mode. Sugai, Sato, and Kurihara¹³ observe three temperature-dependent modes in the Raman spectrum which have frequencies 87, 153, and 197 cm⁻¹ at 25 K. They identify these as symmetric TO amplitude modes of three optic phonon branches coupled to the CDW. The modes we observe at 38, 149, and 194 cm⁻¹ could be the associated antisymmetric phase modes. Another possibility is that the amplitude mode is not symmetric,¹⁴ and hence is ir active. The amplitude mode in (TaSe₄)₂I should be much lower in frequency than 38 cm⁻¹, so this interpretation is unlikely to hold for (TaSe₄)₂I. However, this interpretation is not ruled out for giant FIR modes in other materials.

By completing the excitation spectrum of (TaSe₄)₂I, we have demonstrated conclusively the presence of a large oscillator strength ir active mode of the CDW with frequency between the pinned mode and the Peierls gap. Combined with evidence of similar modes in other CDW systems, our results require a significant modification of the current theory of the CDW excitation spectrum. A detailed study of the effect of impurities on the 38 cm⁻¹ mode in (TaSe₄)₂I is underway.⁸

We thank Professor L. M. Falicov, Dr. P. Bak, and Dr. P. B. Littlewood for useful discussions. This work was supported by the Director, Office of Energy Research, Office of Basic Energy Sciences, Materials Sciences Division of the U. S. Department of Energy under Contract No. DE-AC03-76SF00098 (P.L.R.) and National Science Foundation Grant No. DMR 84000041 (A.Z.). A.Z. also acknowledges support from the Alfred P. Sloan Foundation, and M.S.S. acknowledges support from AT&T Bell Laboratories.

¹G. Travaglini and P. Wachter, Phys. Rev. B **30**, 1971 (1984).

²W. A. Challener and P. L. Richards, Solid State Commun. **52**, 117 (1984).

³H. K. Ng, G. A. Thomas, and L. F. Schneemeyer, Phys. Rev. B

33, 8755 (1986).

⁴P. A. Lee, T. M. Rice, and P. W. Anderson, Solid State Commun. **14**, 703 (1974).

⁵S. Sridhar, D. Reagor, and G. Grüner, Phys. Rev. Lett. **55**,

- 1196 (1985).
- ⁶D. Reagor, S. Sridhar, M. Maki, and G. Grüner, *Phys. Rev. B* **32**, 8445 (1985).
- ⁷R. P. Hall, M. S. Sherwin, and A. Zettl, *Solid State Commun.* **55**, 307 (1985); S. Sridhar (unpublished).
- ⁸M. S. Sherwin, P. L. Richards, and A. Zettl (unpublished).
- ⁹H. P. Geserich, G. Scheiber, M. Dürrieler, F. Lévy, and P. Monceau, *Physica B* **143**, 198 (1986).
- ¹⁰R. J. Cava, P. Littlewood, R. G. Dunn, and E. A. Rietmann, *Phys. Rev. B* **33**, 2439, and references therein. The frequencies in Table I are for temperatures $T/T_p \approx 0.5$.
- ¹¹M. B. Walker, *Can. J. Phys.* **56**, 127 (1978).
- ¹²H. Fujishita, M. Sato, S. Sato, and S. Hoshino, *J. Phys. C* **18**, 1105 (1985).
- ¹³S. Sugai, M. Sato, and S. Kurihara, *Phys. Rev. B* **32**, 6809 (1985).
- ¹⁴P. B. Littlewood (private communication).